www.sciencemag.org/cgi/content/full/320/5883/1620/DC1

Supporting Online Material for

Iron Isotope Fractionation During Magmatic Differentiation in Kilauea Iki Lava Lake

Fang-Zhen Teng,* Nicolas Dauphas, Rosalind T. Helz

*To whom correspondence should be addressed. E-mail: fteng@uark.edu

Published 20 June 2008, *Science* **320**, 1620 (2008)

DOI: 10.1126/science.1157166

This PDF file includes:

Supporting Online Material

SOM1. Whole-rock samples

The Kilauea volcano is located on the southeastern side of the island of Hawaii. Kilauea Iki lava lake lies near the summit of Kilauea volcano, east of its main caldera, and was formed during the 1959 summit eruption of Kilauea volcano (*S1, S2*). Kilauea Iki lava lake was drilled over the period 1960-1988. The quenched drill core samples are instantaneous records of the processes that were active during the cooling of the lava lake. Therefore, the Kilauea Iki lava lake provides an ideal field laboratory for studying magmatic differentiation (*S3*).

The original 1959 Kilauea Iki lava consists of picritic tholeiite and is composed of glass + olivine and chromite crystals, with an average MgO content of 15.43 wt.% (*S2*). Glass compositions in eruption samples range from 6.5 to 10.0 wt.% MgO (*S4*). The olivine phenocrysts include several distinct subpopulations, derived from different levels of Kilauea's plumbing (*S4*). Internal differentiation of the lava lake has produced a variety of rock types from olivine-rich cumulates, through olivine tholeiites, to ferrodiabase and more silicic veins, and large chemical variations with MgO content ranging from 2.37 to 26.87 wt.% (*S4*). Rocks with MgO contents >7.0 wt.% contain olivine phenocrysts in a fine-grained groundmass of glass, clinopyroxene, plagioclase, and opaque minerals in varying amounts (*S4, S5*) and have been affected predominantly by settling of olivine crystals while highly differentiated rocks with MgO contents <7.0 wt.% have been produced by segregation of liquid from within coherent, crystal-rich mushes (*S3,S4*). The quenching temperature of these samples, as estimated by the MgO content of glass (*S6*) or from thermocouple data, ranges from greater than 1216 ^{o}C down to 1055 ^{o}C (*S6*).

Eighteen well-studied samples covering the whole compositional and mineralogical spectrum of the Kilauea Iki lava, including two original eruption samples (Iki-22 and Iki-58) and 16 drill core samples from the interior of the lake, were analyzed to ascertain whether there is any Fe isotopic variation during basaltic differentiation. Nine

of the drill core samples in this study were entirely crystalline when drilled while seven of them (samples KI81-1-239.9, KI81-1-210, KI75-1-139.3, KI67-3-81, KI79-3-158.0, KI67-2-85.7, KI81-5-254.5) consisted of a liquid-crystal "mush" in which the interstitial melt was quenched by the drilling process.

SOM2. Olivine grains

Olivine phenocrysts in the eruption samples preserve a significant amount of internal disequilibrium and are moderately zoned (<3% Fo) with normally and reversely zoned crystals in about equal amounts (*S7*). The presence of variable zoning patterns within samples have been attributed to magma mixing (*S2, S7*). On average, the Fo contents of olivines in the eruption samples are relatively homogenous ($Fo_{86\pm1}$). In contrast, olivines collected by drilling cores from the Kilauea Iki lava lake are all normally zoned, may vary by 5% Fo or more, and have re-equilibrated with the melt during slow cooling (*S7*). The Fo contents of olivines from the lave lake reflect the re-equilibration process and vary significantly with quenching temperatures. Cores of coarse olivines in samples quenched from high temperatures have higher Fo contents than those quenched from lower temperatures (Fig. S1 and Table S3).

Olivine grains have been picked up from two drill core samples. One sample was quenched from relatively high temperature (KI81-5-254.5, 1134 ^{o}C) and the other one was quenched from relatively low temperature (KI75-1-139.3, 1070 ^{o}C) (Table S2). No Fo data are available for these olivine grains but Fo contents in other olivines from the same sample (KI75-1-139.3) have been analyzed (Table S3) and vary from 67 to 76. The Fo contents of olivines from sample KI81-5-254.5 are estimated from the trend in Fig. S1: olivines with quench temperatures of 1135 ^{o}C in the lava lake have a limited range in Fo contents from 79.7 to 81.7. This range is used to represent that of olivines from sample KI81-5-254.5 with a quench temperature of 1134 ^{o}C.

In addition to olivines, sample KI75-1-139.3 contains melt, augite, pigeonite, plagioclase and ilmenite, and sample KI81-5-254.5 contains melt, augite and plagioclase. These additional mineral phases are too small to separate for isotopic analysis.

SOM3. Analytical Method

The whole-rock powders studied here have been used in previous studies *(S3, S4, S8, S9, S10)*. The olivine grains were prepared as follows: Almost pure (>98%) olivine grains were handpicked under a binocular microscope, cleaned with Milli-Q water for 3×10 minutes in an ultrasonic bath, and dried down under a heat lamp before dissolution. Both whole-rock powders and olivine separates were dissolved in a combination of HF-$HClO_4$-HNO_3. Iron was purified on anion exchange resin (AG1-X8 200-400 mesh) in HCl medium by the established procedure of Dauphas et al. (*S11,S12*). Its isotopic composition was analyzed by using a Neptune high-resolution MC-ICPMS installed at the Origins Laboratory, The University of Chicago. The long-term precision, based on replicate analyses of granites, basalts, and chondrites, is ≤0.04‰ (95 % confidence interval).

The accuracy was assessed in several ways. First, Fe isotopic compositions of well-characterized international standards analyzed in our lab agree well with published values (Table S4). Second, IRMM-014 was added to the eluted matrix fractions of several well-characterized samples in quantities that matched the Fe contents of the original samples and these mixtures were then processed through columns and analyzed as unknowns. The results show that these mixtures are isotopically indistinguishable from unprocessed IRMM-014 within 0.03 ‰. Finally, eluted Fe and matrix fractions of four end-member basalt samples were collected and interchanged (KI81-2-88.6 vs. KI81-1-169.9; KI67-2-85.7 vs. KI81-1-210). The results show that these mixtures have Fe isotopic compositions identical to their original samples. These tests demonstrate that we are able to measure both accurately and precisely the Fe isotopic compositions of natural samples at the level of precision reported in Table S4.

SOM4. Rayleigh distillation model in Fig. 4

The equation that governs isotopic fractionation in a Rayleigh distillation process is $(\delta^{56}Fe)_{melt} = [(\delta^{56}Fe)_{initial\ melt} +1000]f^{(\alpha-1)} -1000$, where the fractionation factor is $\alpha = (^{56}Fe/^{54}Fe)_{crystal} / (^{56}Fe/^{54}Fe)_{melt}$, the fraction of Fe remaining in the melt is $f = F \times C_{m,FeO}/C_{i,FeO}$, (i and m subscripts refer to initial and melt, respectively). F is the

fraction of melt remaining and is calculated from the following equation based on the K_2O concentrations of the samples (the concentration of an incompatible element is easily related to the fraction of crystals that have been removed from the system): $C_{m,K2O} = C_{i,K2O} \times F^{(D-1)}$, where $D = K_{crystal} / K_{melt} = 0.04$ (*S13*). $C_{m,FeO}$ is the FeO concentration in the remaining melt and $C_{i,FeO}$ is the Fe concentration in the initial melt.

Since samples with MgO <11 wt% reflect fractional crystallization of olivine , augite, plagioclase and Fe-Ti oxides (*S4*) and no sample with 11 wt% MgO has been analyzed, the sample KI67-3-39 (MgO = 10.73 wt%, total FeO = 11.32 wt%, K_2O = 0.54 wt% and $\delta^{56}Fe$ = 0.11 ‰) is taken to represent the composition of the initial melt in the calculation ($C_{i,FeO}$ = 11.32 wt%). The FeO concentration in the remaining melt, $C_{m,FeO}$, is represented by the FeO concentrations measured in the samples.

SOM5. Mixing model in Fig. 4

The equation that governs mixing of 2 end-members is $\delta^{56}Fe = (\delta^{56}Fe)_1 \times f_1 + (\delta^{56}Fe)_0 \times (1-f_1)$, where f_1 is the fraction of Fe from the end member 1. Dashed lines represent calculated mixing lines between the most magnesian melt and olivines. Olivines from the eruption samples have the highest Fo contents (85-88% Fo (*S7*), corresponding MgO contents of 45.5- 47.7 wt%) and this chemical composition has been used as an end member in the mixing calculation.

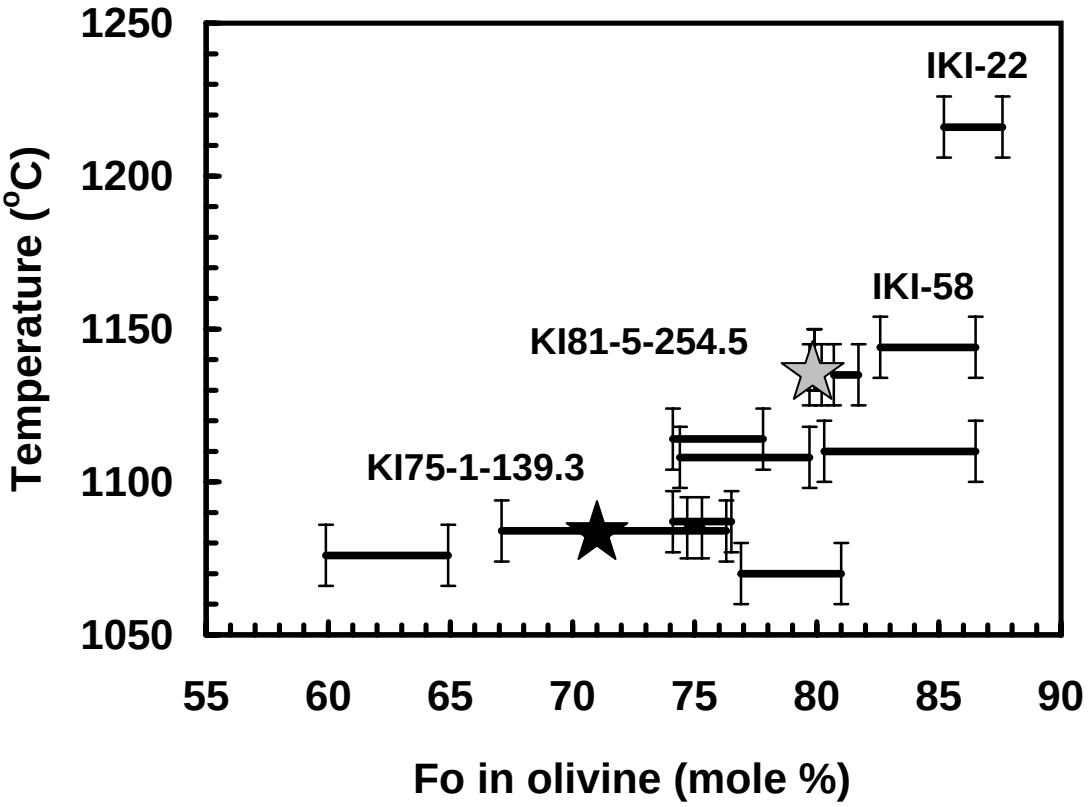

Figure S1.Variations of quench temperatures of whole rocks vs. the range of Fo content in olivine grains. Olivines become progressively more Fe-rich as the temperature decreases and show more scatter in the lower-temperature samples, reflecting partial reequilibration of olivines with evolving residual melts. Data for the maximum and minimum Fo contents in olivine grains from Table S4. The Fo content of sample KI81-5-254.5 is estimated based on the quench temperature of 1134 ^{o}C. See SOM1 and SOM2 for details.

Table S1 Iron isotopic data of whole-rock samples from Kilauea Iki lava lake, Hawaii

Sample	MgO (wt.%)	SiO_2 (wt.%)	K_2O (wt.%)	FeO_{total} (wt.%)	$Fe^{3+}/\sum Fe$	T (^oC)	$\delta^{26}Mg$	$\delta^{56}Fe$	95 % c.i.	$\delta^{57}Fe$	95 % c.i.
KI81-1-169.9	26.87	43.71	0.25	14.80	0.08		-0.34	-0.031	0.027	-0.039	0.038
Cu doping								-0.034	0.024	-0.041	0.047
Rep. Cu doping								-0.024	0.027	-0.044	0.041
Matrix doping								-0.014	0.026	-0.009	0.070
KI81-1-239.9	26.55	44.21	0.20	12.81	0.07	1140		0.031	0.029	0.039	0.028
KI67-3-6.8	25.83	44.63	0.30	12.02	0.16		-0.32	0.050	0.026	0.063	0.045
Cu doping								0.046	0.024	0.084	0.047
KI81-1-210	24.53	44.87	0.21	12.23	0.08	1135	-0.31	0.019	0.027	0.019	0.038
Cu doping								0.014	0.024	0.029	0.047
Rep. Cu doping								0.031	0.027	0.038	0.041
Matrix doping								0.004	0.026	0.001	0.070
IKI-22	19.52	46.68	0.35	11.71	0.12	1216	-0.37	0.069	0.027	0.098	0.038
Cu doping								0.072	0.024	0.108	0.047
KI79-3-150.4	13.51	48.44	0.44	10.54	0.12		-0.41	0.117	0.027	0.176	0.038
Cu doping								0.110	0.022	0.169	0.047
KI75-1-38.9	12.46			11.40	0.12		-0.40	0.100	0.042	0.150	0.064
KI67-3-27.5*	12.01	48.61	0.49	11.16	0.27			0.095	0.039	0.126	0.060
KI75-1-139.3	11.70	48.77	0.52	10.73	0.13	1084		0.127	0.039	0.184	0.060
replicate								0.123	0.032	0.182	0.044
KI67-3-39*	10.73	48.90	0.54	11.32	0.33		-0.39	0.109	0.038	0.176	0.041
IKI-58	8.08	49.91	0.55	11.16	0.21	1144	-0.42	0.209	0.038	0.305	0.041
Cu doping								0.178	0.022	0.264	0.047
KI67-3-81	7.73	49.75	0.63	10.94	0.14	1055	-0.35	0.146	0.029	0.184	0.038
KI75-1-121.5	7.50	50.00	0.64	10.55	0.14		-0.40	0.118	0.039	0.179	0.060
KI75-1-75.2	5.77	50.13	0.79	12.02	0.13		-0.29	0.150	0.039	0.230	0.060
KI79-3-158.0	5.00			12.17	0.20	990		0.193	0.028	0.289	0.041
Cu doping								0.189	0.022	0.293	0.047
KI67-2-85.7	2.60	56.21	1.99	12.03	0.12	1060	-0.35	0.188	0.028	0.288	0.041
Cu doping								0.184	0.022	0.271	0.047
Rep. Cu doping								0.201	0.027	0.289	0.047
Matrix doping								0.206	0.026	0.321	0.070
KI81-2-88.6	2.37	57.07	1.90	11.61	0.19		-0.41	0.224	0.028	0.337	0.041
Cu doping								0.205	0.022	0.310	0.047
Rep. Cu doping								0.224	0.027	0.340	0.041
Matrix doping								0.232	0.026	0.398	0.070
KI81-5-254.5						1134		0.111	0.038	0.141	0.044

The sample number is given first by the drill core number, followed by the depth of the sample in feet: e.g., sample KI81-1-169.9 comes from core KI81-1, 169.9 feet below the surface of the lava lake. Major elemental data from Helz et al. (*S8*) with uncertainties of less than 1% (*S14*); $Fe^{3+}/\sum Fe$ is mole ratio of Fe^{3+} in Fe_2O_3 and total Fe (Fe^{3+} in Fe_2O_3 + Fe^{2+} in FeO), and quench temperatures are estimated for samples consisting of a liquid-crystal "mush" by the MgO geothermometry (*S6*). $\delta^{26}Mg$ data from Teng et al. (*S9*), with an external precision of ±0.1‰. $\delta^{x}Fe = [(^{x}Fe/^{54}Fe)_{sample}/ (^{x}Fe/^{54}Fe)_{standard} -1] \times 1000$, where standard = IRMM-014 and x = 56 or 57); 95 % c.i. stands for 95 % confidence interval of the mean (for 9 replicate analyses of the same solution) and it integrates the long-term reproducibility based on replicate analyses of BHVO-1 standard (*S12*). Cu doping: solutions analyzed by Cu doping method besides sample-standard bracketing method (*S15*); replicate: repeat column chemistry from the same stock sample solution and analyzed by sample-standard bracketing method; Rep. Cu doping; repeat column chemistry from the same stock sample solution analyzed by Cu doping method; Matrix doping: eluted Fe and matrix fractions of four end-member basalt samples were collected and interchanged (KI81-2-88.6 vs. KI81-1-169.9; KI67-2-85.7 vs. KI81-1-210). The mixing solutions were then processed through columns and analyzed as unknowns. Samples marked with "*" are subsolidus samples that have been oxidized by exposure to air in the upper parts of the lake, and therefore their $Fe^{3+}/\sum Fe$ ratios do not reflect initial values.

Table S2 Iron isotopic compositions of olivine grains from Kilauea Iki lava lake, Hawaii

KI81-5-254.5						KI75-1-139.3					
Sample	wt. (mg)	δ^{56}Fe	95 % c.i.	δ^{57}Fe	95 % c.i.	Sample	wt. (mg)	δ^{56}Fe	95 % c.i.	δ^{57}Fe	95 % c.i.
Ol-1	0.56	-0.755	0.032	-1.112	0.044	Ol-1	0.75	-0.253	0.032	-0.406	0.044
Ol-2	0.72	-0.721	0.032	-1.078	0.044	Ol-2	0.47	-0.149	0.032	-0.284	0.044
Ol-3	0.24	+0.032	0.032	+0.007	0.044	Ol-3	0.69	-0.412	0.032	-0.634	0.044
Ol-4	0.37	-0.073	0.032	-0.110	0.044	Ol-4	0.79	+0.017	0.032	-0.137	0.044
Ol-5	0.71	+0.005	0.032	+0.010	0.044	Ol-5	0.49	-0.212	0.032	-0.341	0.044
Ol-6	0.84	-0.134	0.032	-0.225	0.044	Ol-7	0.43	-0.319	0.032	-0.507	0.044
Ol-7	0.60	-0.079	0.032	-0.139	0.044	Ol-8	2.72	-0.164	0.032	-0.294	0.054
Ol-8	0.96	-0.056	0.044	-0.108	0.068	Ol-9	9.40	-0.323	0.029	-0.502	0.050
Ol-9	0.34	+0.085	0.044	+0.104	0.068	Ol-10	1.19	-0.268	0.029	-0.411	0.050
Ol-10	0.49	+0.038	0.044	+0.066	0.068	Ol-11	7.08	-0.271	0.029	-0.413	0.050
Ol-11	1.24	-0.683	0.044	-1.023	0.068	Ol-12	1.36	-0.293	0.029	-0.439	0.050
Ol-12	0.72	-1.103	0.033	-1.680	0.067	Ol-13	1.44	-0.180	0.029	-0.258	0.050
Ol-13	0.42	+0.035	0.033	+0.039	0.067	Ol-14	0.31	-0.210	0.029	-0.321	0.050
Ol-14	0.26	+0.032	0.033	+0.029	0.067	Ol-15	0.72	-0.306	0.029	-0.480	0.050
Ol-15	0.48	-0.419	0.033	-0.620	0.067	Ol-16	0.40	-0.321	0.025	-0.454	0.051
Ol-16	0.46	+0.067	0.033	+0.083	0.067	Ol-17	0.49	-0.316	0.025	-0.473	0.051
Ol-17	0.53	+0.041	0.033	+0.045	0.067	Ol-18	1.28	-0.164	0.025	-0.278	0.051
Ol-18	0.67	-0.154	0.033	-0.236	0.067	Ol-19	0.51	-0.226	0.025	-0.368	0.051
Ol-19	0.41	-0.420	0.034	-0.629	0.060	Ol-20	0.62	-0.205	0.025	-0.316	0.051
Ol-20	1.02	-0.085	0.034	-0.149	0.060	Ol-21	0.47	-0.240	0.025	-0.374	0.051
Ol-21	1.42	+0.022	0.034	+0.014	0.060	Ol-22	1.02	-0.238	0.025	-0.401	0.051
Average		-0.206	0.155	-0.320	0.230	Average		-0.241	0.040	-0.388	0.074

95 % c.i. stands for 95 % confidence interval of the mean (for 9 replicate analyses of the same solution) and it integrates the long-term reproducibility based on replicate analyses of BHVO-1 standard (*S12*).

Table S3 Major element compositions of olivines from Kilauea Iki lava lake

Sample		SiO_2 (wt.%)	FeO (wt.%)	MgO (wt.%)	Fo (mole%)	T (^oC)
KI67-3-83.8	Max	35.5	31.4	32.6	64.9	1076
	Min	35.1	35.0	29.3	59.9	
KI75-1-139.3	Max	37.7	22.1	39.8	76.3	1084
	Min	36.8	29.3	33.6	67.1	
KI75-1-143.8	Max	38.2	21.0	41.2	77.8	1114
	Min	37.6	24.2	38.9	74.1	
KI79-3-166.1*	Max	38.9	17.9	43.0	81.0	1070
	Min	38.2	21.5	40.0	76.9	
KI79-3-172.9	Max	38.8	18.9	41.7	79.7	1108
	Min	37.2	23.7	38.6	74.4	
KI79-3-172.9*	Max	39.5	12.7	45.7	86.5	1110
	Min	38.9	18.2	41.6	80.3	
KI81-1-186.7	Max	38.0	22.7	38.7	75.3	1085
	Min	38.0	23.2	38.4	74.7	
KI81-1-205.4	Max	39.2	18.5	42.1	80.2	1135
	Min	37.8	19.0	42.0	79.7	
KI81-1-209.8*	Max	38.9	17.0	42.7	81.7	1135
	Min	38.8	17.8	41.9	80.7	
KI81-1-219.8	Max	38.3	19.0	42.2	79.9	1140
	Min	37.6	18.8	42.0	79.9	
KI81-1-306.7	Max	37.4	21.9	40.0	76.5	1087
	Min	36.9	24.0	38.5	74.1	
IKI-58	Max	40.0	13.0	46.6	86.5	1144
	Min	38.8	16.5	43.9	82.6	
IKI-22	Max	39.9	12.1	47.8	87.6	1216
	Min	39.4	14.2	45.9	85.2	

Major element compositions are analyzed by electronic microprobe from Helz (unpublished data). * Data are taken from Scowen et al. (*S16*). Fo is the mole fraction of forsterite in olivine (forsterite + fayalite). Quench temperatures are estimated by the MgO geothermometry (*S6*).

Table S4 Iron isotopic compositions of basalts, geostandards and meteorites analyzed during this study

Sample	Description	δ^{56}Fe	95 % c.i.	δ^{57}Fe	95 % c.i.
BHVO-1	Basalt (Kilauea, Hawaii)	+0.111	0.022	+0.156	0.033
Replicate		+0.100	0.033	+0.140	0.055
Average		+0.109	0.021	+0.154	0.033
T4D2#1	Basalt (Loihi, Hawaii)	+0.047	0.030	+0.073	0.050
T4D3#3	Basalt (Loihi, Hawaii)	+0.067	0.030	+0.099	0.050
T4D3#7	Basalt (Loihi, Hawaii)	+0.056	0.030	+0.118	0.050
BCR-1	Basalt (Columbia River, Oregon)	+0.088	0.028	+0.111	0.045
VS-90-56	Basalt (American-Antarctic ridge)	+0.179	0.028	+0.255	0.045
DTS-2	Dunite (Twin Sisters Mountain, WA)	-0.006	0.022	-0.004	0.040
AC-E	Granite (Ailsa Craig island, Scotland)	+0.330	0.032	+0.497	0.044
IF-G	BIF (Isua, Greenland)	+0.633	0.030	+0.945	0.050
Allende	Chondrite (CV3)	-0.010	0.030	-0.010	0.050

Replicate: repeat column chemistry from the same stock sample solution and analyzed by sample-standard bracketing method; 95 % c.i. stands for 95 % confidence interval of the mean (for 9 replicate analyses of the same solution) and it integrates the long-term reproducibility based on replicate analyses of BHVO-1 standard (*S12*).

References

S1. D. H. Richter, J. P. Eaton, K. J. Murata, W. U. Ault, H. L. Krivoy, *Chronological narrative of the 1959-60 eruption of Kilauea volcano, Hawaii*, U.S. Geol. Surv. Prof. Paper 537-E (1970), pp. 73.

S2. T. L. Wright, *Geological Society of America Bulletin* 84, 849 (1973).

S3. R. T. Helz, H. Kirschenbaum, J. W. Marinenko, *Geological Society of America Bulletin* 101, 578 (1989).

S4. R. T. Helz, in *Magmatic Processes: Physiochemical Principles* B. O. Mysen, Ed. (Geochem. Soc. Spec. Publ. 1, 1987) pp. 241-258.

S5. D. H. Richter, J. G. Moore, *U.S.G.S. Prof. Paper*, 537 (1966).

S6. R. T. Helz, C. R. Thornber, *Bulletin of Volcanology* 49, 651 (1987).

S7. R. T. Helz, *U.S.G.S. Prof. Paper* 1350, 691 (1987).

S8. R. T. Helz, H. Kirschenbaum, J. W. Marinenko, R. Qian, *U.S.G.S. Open File Report*, 94 (1994).

S9. F.-Z. Teng, M. Wadhwa, R. T. Helz, *Earth and Planetary Science Letters* 261, 84 (2007).

S10. P. B. Tomascak, F. Tera, R. T. Helz, R. J. Walker, *Geochimica et Cosmochimica Acta* 63, 907 (1999).

S11. N. Dauphas *et al.*, *Analytical Chemistry* 76, 5855 (2004).
S12. N. Dauphas, A. Pourmand, F.-Z. Teng, *Chemical Geology*, In review (2008).
S13. H. Taura, H. Yurimoto, K. Kurita, S. Sueno, *Physics and Chemistry of Minerals* 25, 469 (1998).
S14. H. Kirschenbaum, *U.S.G.S. Bull.* 1547, 55p. (1983).
S15. F. Albarede, B. L. Beard, in *Geochemistry of Non-Traditional Stable Isotopes* C. M. Johnson, B. L. Beard, F. Albarede, Eds. (Miner. Soc. of America, 2004), vol. 55, pp. 113-152.
S16. P. A. H. Scowen, P. L. Roeder, R. T. Helz, *Contributions to Mineralogy and Petrology* 107, 8 (1991).